Neuron
Report

Retromer Mediates a Discrete Route of Local Membrane Delivery to Dendrites

Regina Wai-Yan Choy,[1,4] Minjong Park,[1,4] Paul Temkin,[2] Bruce E. Herring,[3] Aaron Marley,[1] Roger A. Nicoll,[3] and Mark von Zastrow[1,2,3,*]
[1]Department of Psychiatry
[2]Program in Cell Biology
[3]Department of Cellular & Molecular Pharmacology
University of California at San Francisco School of Medicine, San Francisco, CA 94158, USA
[4]Co-first authors
*Correspondence: mark.vonzastrow@ucsf.edu
http://dx.doi.org/10.1016/j.neuron.2014.02.018

SUMMARY

A fundamental and still largely unresolved question is how neurons achieve rapid delivery of selected signaling receptors throughout the elaborate dendritic arbor. Here we show that this requires a conserved sorting machinery called retromer. Retromer-associated endosomes are distributed within dendrites in ~2 μm intervals and supply frequent membrane fusion events into the dendritic shaft domain immediately adjacent to (<300 nm from) the donor endosome and typically without full endosome discharge. Retromer-associated endosomes contain β-adrenergic receptors as well as ionotropic glutamate receptors, and retromer knockdown reduces extrasynaptic insertion of adrenergic receptors as well as functional expression of AMPA and NMDA receptors at synapses. We propose that retromer supports a broadly distributed network of plasma membrane delivery to dendrites, organized in micron-scale axial territories to render essentially all regions of the postsynaptic surface within rapid diffusion distance of a local exocytic event.

INTRODUCTION

Neural development and plasticity processes require dynamic and local remodeling of the plasma membrane of dendrites (Kennedy and Ehlers, 2011). The dendritic arbor is an elaborate neuronal surface domain, often extending long distances from the cell body and including thousands of synaptic specializations. Dendrites contain a large amount of endocytic membrane (Cooney et al., 2002) and endosomes have been recognized for many years to play a major role in regulating postsynaptic responsiveness (Carroll et al., 2001). A key question that is largely unanswered, and has remained a fundamental conceptual problem since the initial discoveries that specific signaling receptors are rapidly removed from synapses by activity-dependent lateral redistribution (Lissin et al., 1999) and endocytosis (Carroll et al., 1999), is how such receptors are conversely delivered out to the expansive dendritic surface with comparable speed.

Receptors can be delivered to dendrites via long-range lateral diffusion from the cell body (Adesnik et al., 2005) or by direct exocytic discharge of recycling endosomes within spines (Kennedy et al., 2010). Long-range diffusion is fundamentally limited in rate (Berg and Purcell, 1977) and exocytosis in spines is inherently restricted by anatomy. A third delivery route is via membrane insertion into the shaft domain of dendrites, outside of spines but often in close proximity, producing transient regions of locally increased surface receptor concentration that drive subsequent spread into adjacent extrasynaptic and synaptic regions by mass action and short-range lateral diffusion. This delivery route, postulated long ago (Passafaro et al., 2001), was first directly demonstrated for G protein-coupled receptors (GPCRs) that function largely outside of synapses (Yudowski et al., 2006). Accumulating evidence suggests that it also plays a major role in mediating synaptic delivery of ligand-gated ion channels both in dissociated neurons (Araki et al., 2010; Opazo and Choquet, 2011; Yudowski et al., 2007) and brain slice cultures (Makino and Malinow, 2009; Patterson et al., 2010). However, little is known about the trafficking machinery underlying this third route of postsynaptic membrane delivery.

We gained insight to this question through study of retromer, a deeply conserved heteromeric protein complex that assembles on a subdomain of the endosome-limiting membrane (Bonifacino and Hurley, 2008) and was so named for its first-recognized function in mediating "retrograde" trafficking of selected proteins from endosomes to a Golgi-like compartment in yeast (Seaman et al., 1998). Retromer subunits are highly expressed in brain and mediate retrograde trafficking from endosomes located in neuronal processes to Golgi elements located in the cell body (Bhalla et al., 2012; Choy et al., 2012). The present results identify a discrete and additional function of the neuronal retromer in mediating the third surface delivery route by supporting local membrane insertion in dendrites.

RESULTS

Retromer-Associated Endosomes Are Broadly Distributed throughout the Dendritic Shaft

Because rapid recycling of β2ARs in nonneural cells depends on retromer (Temkin et al., 2011), and the same cytoplasmic sorting sequence directs endosome-to-plasma membrane traffic of receptors in neurons (Yu et al., 2010), we wondered whether

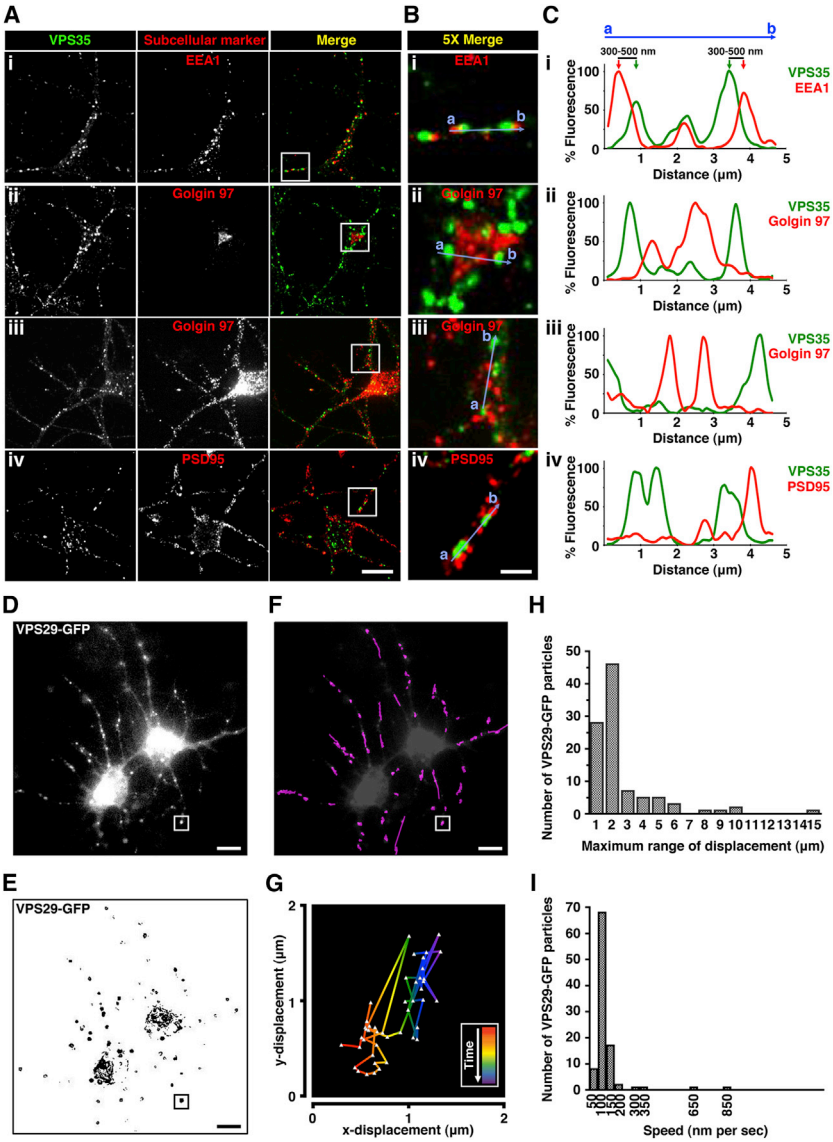

Figure 1. Retromer-Associated Endosomes Are Dynamic and Move Locally in Dendrites

(A) Representative confocal images showing localization of endogenous VPS35 (green) and subcellular markers (red) including: (i) early endosomal marker EEA1, *trans*-Golgi network marker Golgin 97 in both the (ii) cell body and (iii) dendrites, and (iv) postsynaptic density protein PSD95, in striatal neuron culture. Golgin 97 was rendered at higher sensitivity in (iii), saturating the cell body, due to much lower concentration in dendrites. Scale bar, 10 μm. (B) Regions outlined by white squares in merged images in (A) are shown at a higher magnification. Scale bar, 2 μm. (C) Fluorescence intensity trace of VPS35 (green) and subcellular markers (red) scanning across corresponding blue lines from (a) to (b) as indicated in (B), normalized to the maximum intensity. (D) Live-cell imaging of neurons expressing VPS29-GFP using wide-field fluorescence microscopy. Shown is a frame from a representative time-lapse image series (see Movie S1). Images were acquired every 3 s. Scale bar, 10 μm. (E) Time series from (D) were grayscale inverted, and individual VPS29-GFP particles were shown as black puncta. Scale bar, 10 μm. (F) Individual VPS29-GFP particles in dendrites were tracked as purple traces by analyzing 100 particles. Traces in dendrites are superimposed on the image shown in (D), except at lower contrast and not showing trajectories with the cell body for clarity. Scale bar, 10 μm. (G) An example of the trajectory of an individual VPS29-GFP particle as indicated by the white square in (F). Red represents the start of the tracking and purple represents the end of the tracking. (H) Frequency distribution analysis of the maximum range of displacement by VPS29-GFP in dendrites (analyzed from 100 particles). (I) Frequency distribution analysis of the average speed of VPS29-GFP movement between 3 s frames in dendrites (analyzed from 100 particles).

retromer might function in β2AR surface delivery to dendrites. We chose to investigate this question in medium spiny neurons because they produce elaborate dendritic arbors, express endogenous β2ARs throughout synaptic and extrasynaptic regions, and can replace essentially their entire surface receptor complement through endocytic recycling within minutes (Aoki et al., 1987; Yu et al., 2010). To localize retromer in fixed cells, we examined endogenous VPS35 immunoreactivity as a marker of the assembled complex (Arighi et al., 2004). VPS35 localized in a punctate pattern characteristic of retromer in the cell body and dendrites. In both regions, VPS35 overlapped early endosome membranes marked by early endosome antigen 1 (EEA1) (Figure 1A, row i). VPS35 and EEA1 signals were not completely superimposed but appeared in close register, with respective centroids typically offset by ~400 nm (Figures 1B and 1C, row i), consistent with organization of retromer on a subdomain of the early endosome membrane as described previously in nonneural cells (Arighi et al., 2004; Temkin et al., 2011). We did not observe significant overlap of VPS35 with the endogenous Golgi marker Golgin97 (Figures 1A–1C, rows ii and iii; Figure S1A) or the synaptic marker PSD95 (Figure 1C, row iv; Figure S1C), but membrane concentration in dendrites was so high that essentially every postsynaptic density and peripheral Golgi element was located within 1–2 μm of at least one retromer-associated endosome.

Retromer-Associated Endosomes Move Rapidly in Local Regions of the Dendrite

To examine retromer in live neurons, we expressed a GFP-tagged version of VPS29 (VPS29-GFP) that labels the assembled retromer in nonneural cells (Arighi et al., 2004) and verified this in striatal neurons (Figures S1B and S1D). Wide-field imaging captured large portions of the dendritic arbor in a single focal plane (Figure 1D; Movie S1). Some retromer-associated endosomes moved long distances in dendrites, consistent with retrograde trafficking described previously (Bhalla et al., 2012; Choy et al., 2012), but analysis of individual trajectories (Figure 1E)

revealed that the majority moved in limited axial regions. These local trajectories were sufficiently dense that, when overlapped, they effectively filled the dendrite (Figure 1F). On average, retromer-associated endosomes moved in ~2 μm axial regions at ~100 nm/s (Figures 1G–1I), sufficient to fully cover the dendrite length in aggregate within ~20 s.

β2ARs Traverse Retromer-Associated Endosomes after Ligand-Induced Endocytosis

Recombinant β2ARs localized in the plasma membrane of dendrites in the absence of agonist, internalized robustly within 5 min after application of the agonist ligand isoproterenol and localized to retromer-associated endosomes after endocytosis (Figure 2A, row i). β2AR immunoreactivity in individual endosomes extended beyond the VPS35-labeled portion (Figure 2B, see arrows), suggesting that only a fraction of endosome-localized β2ARs partitioned into the retromer domain. This is consistent with studies of β2AR trafficking in nonneural cells, where receptors localize within and outside of retromer tubules extending from endosomes (Puthenveedu et al., 2010; Temkin et al., 2011). Similar β2AR localization was observed after 30 min of continuous exposure to isoproterenol (Figure 2A, row ii), sampling a steady state of repeated rounds of β2AR endocytosis and recycling (Yu et al., 2010; Yudowski et al., 2006). β2ARs localized to endosomes (Figure 2A, row iii) but not detectably to Golgi elements (Figure 2A, row iv; Figure S2), and β2AR and VPS29-GFP spots moved coordinately in wide-field (Figures 2D and 2E) and confocal (Figures 2F and 2G; see also Movie S2) image series. β2AR localization to retromer-associated endosomes was agonist dependent, but retromer-associated endosomes were present in dendrites irrespective of agonist application (Figure S2G).

β2AR Delivery from Endosomes to the Dendritic Surface Requires Retromer

To ask whether retromer impacts surface delivery of β2ARs from endosomes in neurons, we used RNA interference to deplete endogenous VPS35, an essential component of the retromer complex (Arighi et al., 2004; Seaman et al., 1998). Neurons were transfected with a plasmid encoding both epitope-tagged β2AR and a designed short hairpin RNA (shRNA) duplex, assuring coincident cellular expression of the indicated shRNA with tagged β2ARs. In neurons expressing a nontargeting ("control") duplex, retromer marked by endogenous VPS35 was detected in bright puncta on endosomes throughout the cell body and dendrites (Figure 3A, top row). In neurons expressing a targeting ("VPS35 KD") duplex, retromer puncta were markedly depleted even though bright labeling was evident in neighboring untransfected neurons (Figure 3A, bottom row; quantification in Figure 3B). We then examined trafficking of coexpressed β2ARs using a previously described assay (Yu et al., 2010) (Figure 3C). Retromer depletion did not prevent basal surface expression of β2ARs (Figure 3E, rows i and iv; surface receptors appear yellow in the merge) or their agonist-induced endocytosis (rows ii and v, green signal in the merge). However, retromer depletion markedly reduced β2AR recycling after agonist removal, indicated by internalized β2AR signal (green) remaining specifically in VPS35 KD neurons (rows iii and vi). Quantification by fluorescence ratio imaging revealed ~3-fold inhibition of β2AR recycling, which was rescued by expression of an shRNA-resistant VPS35 construct (Figure 3D; Figure S3).

β2ARs Are Inserted to the Surface of Dendrites by Shaft-Directed Membrane Fusion Occurring in Close Proximity to Retromer-Associated Endosomes

We next investigated the route of β2AR recycling from retromer-associated endosomes. Discrete receptor-containing surface insertion events were detected by dequenching of superecliptic pHluorin (SEP) fused to the β2AR ectodomain (Sankaranarayanan et al., 2000; Yudowski et al., 2006). We modified this method by fusing an HA epitope in tandem with the SEP (SEP-HA-β2AR) to simultaneously detect inserted (SEP) and internal (HA) β2ARs (Figure 4A). Dual imaging was carried out using total internal reflection fluorescence microscopy (TIR-FM) at 10 Hz to resolve individual SEP puffs representing β2AR-containing insertion events before their dissipation by lateral diffusion and placing a beam splitter in the emission light path to simultaneously acquire the anti-HA channel.

TIR-FM achieves sensitive detection of insertion events in the dendritic shaft (Yudowski et al., 2006) but is limited in practical illumination depth to 50–150 nm (Jaiswal and Simon, 2007; Steyer and Almers, 2001), precluding examination of synaptic specializations protruding from the top surface of dendrites in culture. β2AR-containing insertion events appeared as characteristic puffs of SEP fluorescence in a single 100 ms frame that dissipated with variable kinetics thereafter (Yu et al., 2010; Yudowski et al., 2006) (Figure 4B; Movie S3). SEP-marked β2AR insertion events overlapped a spot of internal receptor fluorescence detected in the corresponding HA channel, identifying a candidate donor compartment (Figure 4C, the frame in which the SEP puff appeared is assigned $t = 0$). These dithered locally before an insertion event (Figure 4C, $t < 0$), as expected for retromer-associated endosomes. Surprisingly, many also remained intact after a discrete SEP puff appeared and dispersed (Figure 4C, $t > 0$). This behavior was typical (>80% of events observed), suggesting that surface insertion of β2ARs to the shaft domain of dendrites often occurs without full discharge of the donor membrane compartment.

β2AR-containing donor compartments corresponded to retromer-associated endosomes, as indicated by dual imaging of SEP-β2AR puffs relative to the retromer marker VPS29-mCherry. By replacing the emission beam splitter with a fixed dual band-pass filter, and separating SEP (inserted β2ARs) and mCherry (retromer domain) signals by toggling laser excitation wavelength at 20 Hz (achieving an effective dual channel acquisition rate of 10 Hz), retromer domains marked by a spot of VPS29-mCherry fluorescence were found to overlap associated SEP puffs to the diffraction limit (Figure 4D; Movie S4). We quantified these results by scoring in sequential image series whether each observed β2AR insertion event (SEP puff) colocalized with a retromer domain (VPS29-mCherry spot) in frames both immediately preceding (i.e., 50 ms before) and following (i.e., 50 ms after) the insertion event; according to this analysis, 61% ± 10% of β2AR-containing insertion events coincided with a visible retromer domain (overall insertion frequency of 10 ± 4 events/min/microscopic field, each including on average 60 μm of dendrite length; n = 30 microscopic fields collected from five

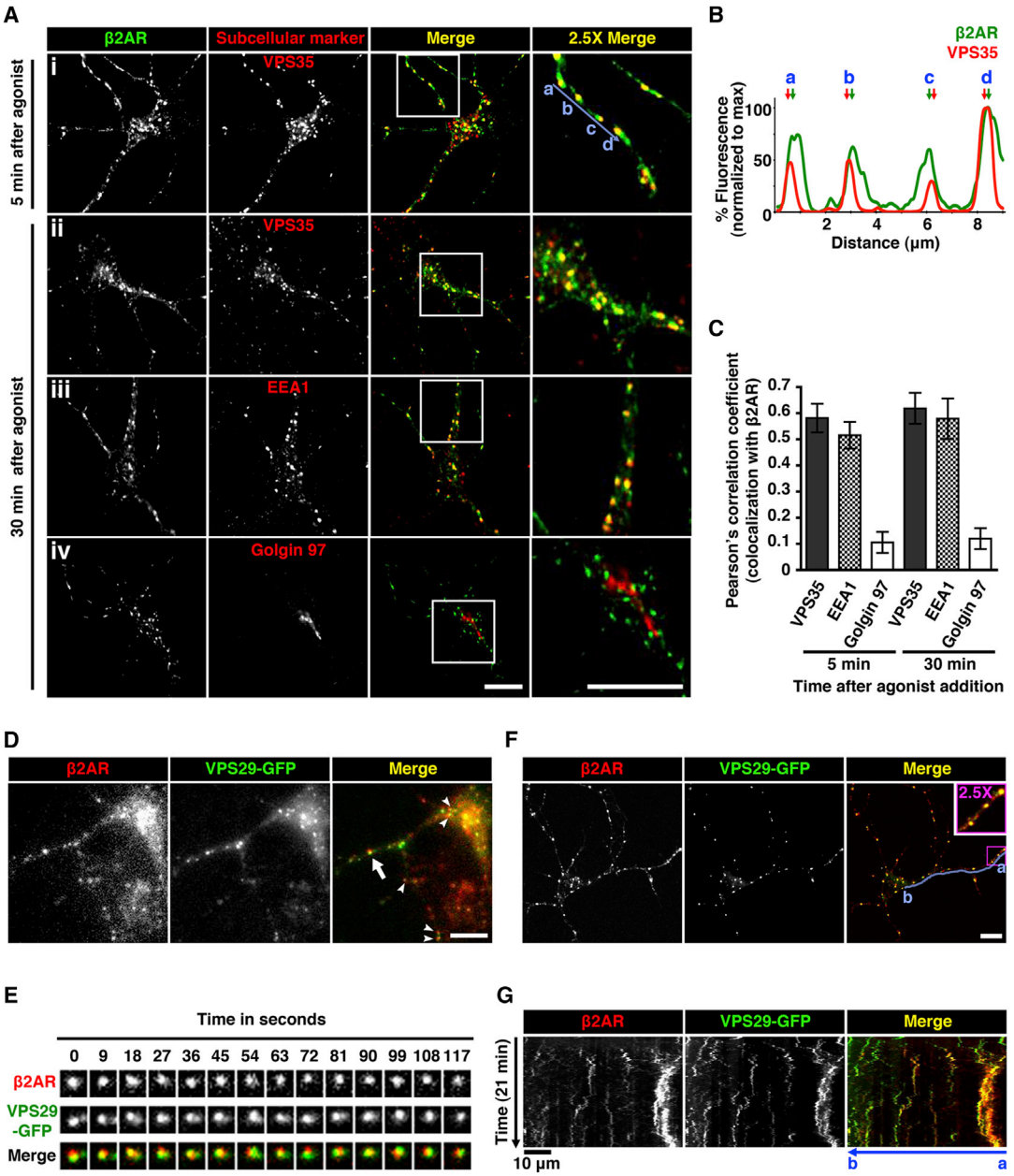

Figure 2. Internalized β2ARs Traverse Retromer-Associated Endosomes

(A) Neurons expressing HA-β2AR surface labeled with a fluorescently conjugated anti-HA antibody were imaged after 5 min and 30 min of adrenergic agonist (1 μM isoproterenol) exposure. Shown are representative confocal images of localization of HA-β2AR (green) and endogenous subcellular markers (red). Regions outlined by white squares in merged images are enlarged in the right column. Scale bars, 10 μm. (B) Fluorescence intensity trace of HA-β2AR (green) and endogenous VPS35 (red) normalized to the maximum intensity, scanning across multiple retromer-associated endosomes as indicated by (a) to (d) (blue line) in (A) after 5 min of agonist treatment. Arrows indicate corresponding peaks of the fluorescence channels. (C) Quantitative colocalization analysis of HA-β2AR with subcellular markers after agonist treatment. Pearson's correlation coefficient was obtained by analysis of at least 20 cells. Error bars indicate SD of the individual determinations. (D) Frame from a representative time-lapse image series, using wide-field fluorescence microscopy, of neurons coexpressing HA-β2AR (red) and VPS29-GFP (green) after 10 min of agonist treatment. Arrow and arrowheads denote examples of colocalization of internalized HA-β2AR with VPS29-GFP. Scale bar, 10 μm. (E) Multiple frames from a representative time series of a HA-β2AR (red) and VPS29-GFP (green)-containing endosome as indicated by the arrow in (D). (F) Live-cell imaging of neurons coexpressing HA-β2AR (red) and VPS29-GFP (green) after 5 min of agonist treatment using confocal microscopy. Shown is a frame from a representative time-lapse image series (see Movie S2). Region outlined by the purple square in the merged image is enlarged and shown in the inset. Scale bar, 10 μm. (G) Kymographs of the movement of FLAG-β2AR (red) and VPS29-GFP (green) from the time series in (F). Kymographs drawn along the dendrite across multiple β2AR-containing retromer-associated endosomes (blue line from a to b) represent movement over time. Images were acquired every 5 s, and agonist was added after 1 min. Scale bars for the x axis and y axis represent 10 μm and 5 min, respectively. Dynamic VPS29-GFP puncta were visible throughout the time series but β2AR localization to these endosomes was stimulated by agonist (Movie S2 shows an entire time series).

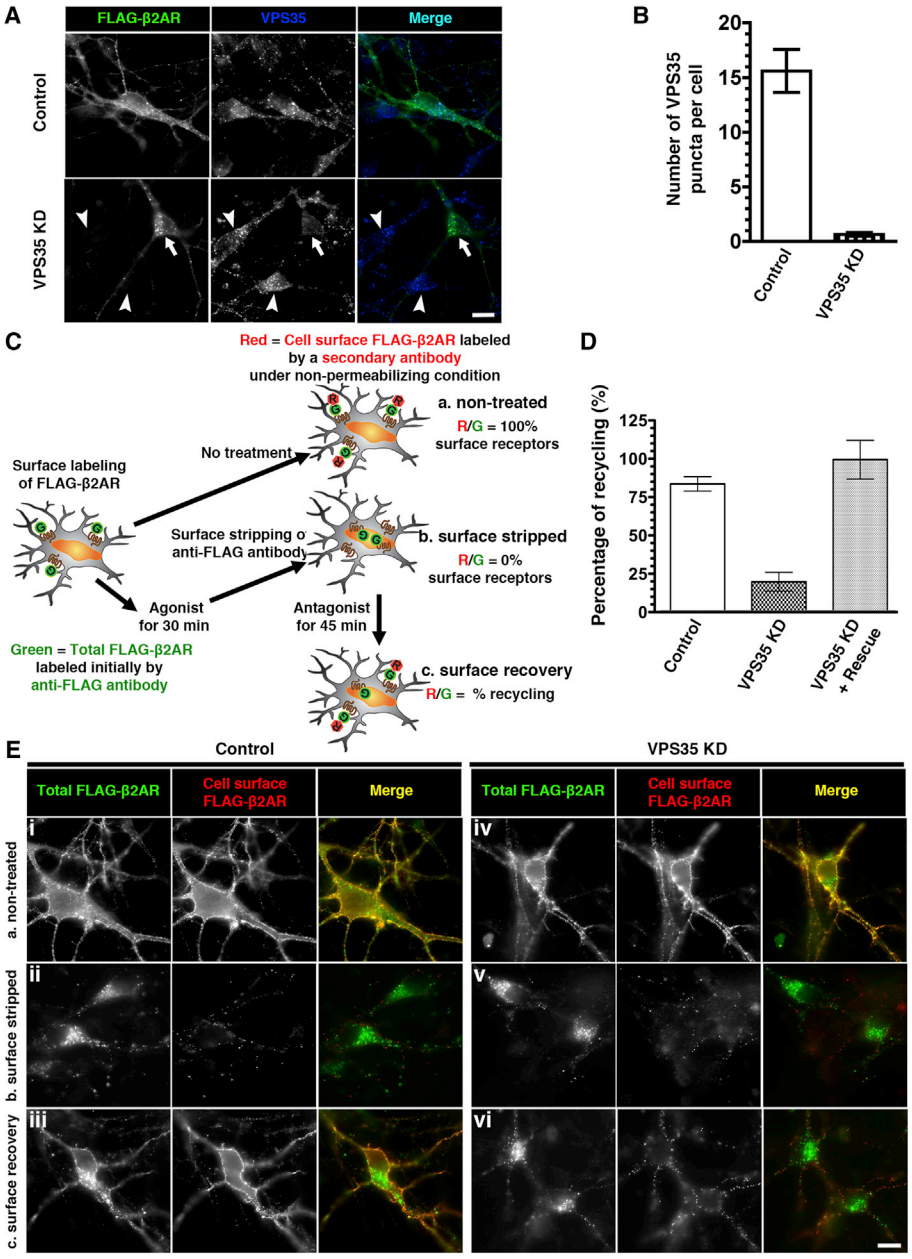

Figure 3. β2AR Recycling in Neurons Is Retromer Dependent

(A) Depletion of endogenous VPS35 in neurons by transfecting a plasmid coencoding FLAG-β2AR together with an shRNA duplex targeting endogenous VPS35 (VPS35 KD) or a nonsilencing (control) duplex. Distinct puncta of VPS35 were present in the control cells (top). Reduced punctate retromer staining was observed in neurons expressing the VPS35 KD construct (bottom row, arrow indicates a representative example neuron), whereas bright staining was observed in neighboring untransfected neurons (arrowheads). Scale bar, 10 μm. (B) Quantification of the number of VPS35 puncta in the control and VSP35 KD cells by analysis of at least 20 cells in each condition. Error bars indicate SD across individual determinations. (C) Schematic of quantitative β2AR recycling assay using dual-color labeling and fluorescence ratiometric image analysis. Neurons expressing FLAG-β2AR surface labeled with a fluorescently conjugated anti-FLAG antibody (green) were subjected to three sets of conditions in parallel: (a) control with no treatment (represents 100% surface receptors); (b) 30 min of agonist (isoproterenol treatment followed by surface stripping of residual β2AR-bound antibody (represents 0% surface receptors); and (c) 45 min of adrenergic antagonist (alprenolol) treatment following the same procedure as in condition (b) to monitor cell surface recovery of β2AR. Ratiometric image analysis was done by calculating the ratio of fluorescence intensity of nonpermeabilizing staining of cell surface β2AR by a secondary antibody (red) to the overall intensity of β2AR initially labeled with anti-FLAG antibody on the plasma membrane (green). The percentage of recycling was calculated as described in Experimental Procedures. (D) Quantification of the percentage of β2AR recycling to the cell surface in control, VPS35 KD, and rescue conditions as determined by fluorescence ratiometric image analysis of at least 75 cells per condition across three independent sets of experiments, using the dual-color labeling method described in (C). Error bars indicate SD. (E) Representative wide-field fluorescence images of β2AR recycling assay in the control and VSP35 KD cells using dual-color labeling method as described in (C) (scale bar, 10 μm).

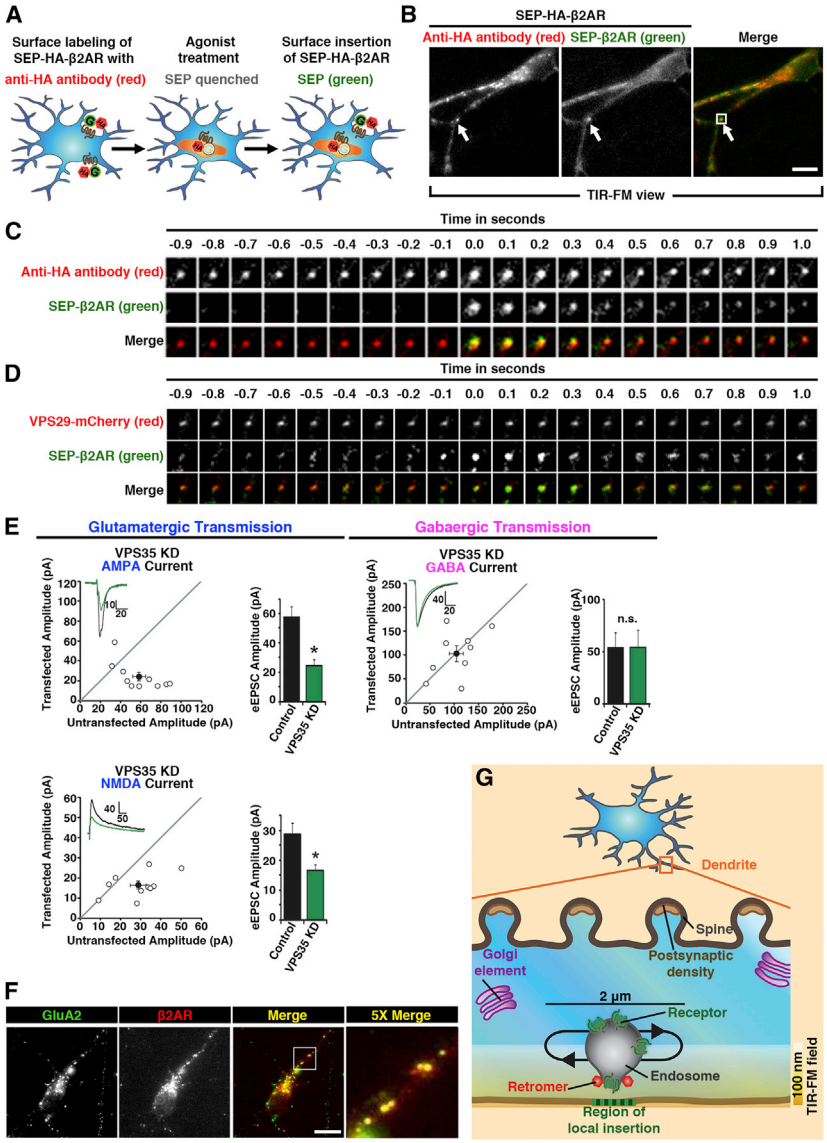

Figure 4. Retromer Underlies Local Membrane Insertion to the Dendritic Shaft and Contributes to Functional Surface Expression of Glutamate Receptors at Synapses

(A) Schematic of method for simultaneously labeling SEP-HA-β2AR surface insertion events and endosomes using SEP (green) and anti-HA (red) fluorescence. SEP puffs occur upon β2AR insertion to the plasma membrane while the red Alexa Fluor conjugated to anti-HA is not significantly pH dependent, revealing the adjacent receptor-containing endosome. (B) A frame from a representative TIR-FM image series of SEP and HA fluorescence, acquired using the scheme diagramed in (A), simultaneous channel capture, and a relatively "deep" angle to illuminate a significant portion of ventral dendroplasm. A representative SEP puff is indicated by arrow. Scale bar, 10 μm. See also Movie S3. (C) Higher-magnification view of multiple frames from the area indicated. (D) TIR-FM image series showing SEP puffs relative to retromer domains marked by VPS29-mCherry, acquired under similar conditions except using sequential imaging of paired channels at 20 Hz and a relatively "shallow" angle to illuminate little ventral dendroplasm. See also Movie S4. (E) Electrophysiological analysis of VPS35 KD effects on AMPA-, NMDA-, and GABA-mediated synaptic currents in hippocampal slice culture. Scatterplots show amplitudes of AMPAR and NMDAR eEPSCs and $GABA_AR$ eIPSCs for single pairs of neurons (open circles) and mean ± SEM (filled circles) across all neuron pairs collected. The scatterplots represent data obtained from slice cultures 6 days after transfection with the VPS35 shRNA-EGFP construct (current amplitude plotted on the ordinate) relative to an adjacent nontransfected neuron (current amplitude plotted on the abscissa). Insets show sample current traces from control (black) and transfected (green) cells. Bar graphs summarize mean ± SEM. AMPAR and NMDAR eEPSC and $GABA_AR$ eIPSC amplitudes represented in the respective scatterplots (*$p < 0.05$). (F) Labeling of overlapping endosomes by endogenous GluA2 and FLAG-β2AR, after coincubation of neurons in dissociated culture with anti-GluA2 and anti-FLAG antibodies for 20 min in Neurobasal medium supplemented with 1 μM isoproterenol. (G) Schematic of an enlarged view of a dendrite showing the localization of different subcellular compartments relative to retromer-associated endosomes that move locally within a short range of 2 μm. Surface delivery of β2AR from endosomes to the plasma membrane occurs very locally relative to the retromer domain, and the retromer domain is located very close to the location of surface insertion because it is readily visualized in the TIR-FM illumination field and effectively overlaps the location of the retromer-associated endosome in x and y dimensions.

separate experiments). Given an estimated evanescent illumination depth of ~100 nm (Steyer and Almers, 2001) and a (diffraction-limited) x-y spatial resolution of ~200 nm, this suggests that membrane fusion events mediating shaft-directed surface insertion of β2ARs in dendrites typically occur within ~300 nm of a local retromer-associated endosome and of its retromer domain.

Retromer Is Required for Functional Surface Expression of Synaptic Glutamate Receptors

While β2ARs offer significant experimental advantages for imaging discrete trafficking events, they represent only one of many itinerant signaling receptors in dendrites. To investigate whether retromer is important to other postsynaptic receptors, we focused on ligand-gated ion channels that mediate fast synaptic transmission. The shRNA strategy used in dissociated culture was modified for coexpression of EGFP (rather than the tagged β2AR) by biolistic transfection (rather than electroporation) in cultured hippocampal slices, as described previously (Herring et al., 2013). Synaptic AMPA and NMDA excitatory postsynaptic currents (EPSCs) were significantly reduced in VPS35 knockdown neurons but GABA inhibitory postsynaptic currents (IPSCs) were not detectably affected (Figure 4E). Further, endogenous AMPA receptors marked by GluA2 immunoreactivity internalized to endosomes also containing tagged β2ARs in striatal (Figure 4F) and hippocampal (data not shown) neurons. Thus,

retromer function in postsynaptic membrane delivery does not appear to be limited to the β2AR or to medium spiny neurons.

DISCUSSION

The present results identify an essential function of the neuronal retromer machinery in supporting a rapid and local mechanism of surface membrane insertion to the shaft domain of dendrites, revealing an additional role of retromer in neurons and a discrete route of postsynaptic membrane delivery (Figure 4G). Retromer is essential for rapid insertion of β2ARs that are widely distributed in dendrites and most abundant outside of synapses (Aoki et al., 1987), as well as for appropriate functional surface expression of AMPA and NMDA receptors at synapses. This suggests that retromer-dependent trafficking underlies delivery of various signaling receptors to the surface of dendrites and to both extrasynaptic and synaptic sites.

β2ARs are sorted in retromer-associated endosomes by binding to sorting nexin 27 (SNX27), which recognizes the β2AR cytoplasmic tail and associates with retromer via multiple interactions (Lauffer et al., 2010; Steinberg et al., 2013; Temkin et al., 2011). SNX27 recognizes a number of other membrane proteins in addition to adrenergic receptors (Steinberg et al., 2013) and can promote surface expression of AMPA and NMDA receptors in neurons (Wang et al., 2013). Thus, the present results suggest a unified biochemical principle for receptor selection into the local delivery route, but they leave its physical basis unclear. Because surface insertion events are located very close to retromer-associated endosomes, it is difficult to determine with certainty if they occur by formation and full fusion of a small vesicular intermediate (not resolved in our images) or by direct but incomplete endosome-to-plasma membrane transfer (Ryan, 2003; Taraska and Almers, 2004). We note, however, that some insertion events showed SEP dequenching overlapping only a portion of the candidate donor compartment, whereas others showed dequenching apparently throughout (Movies S3 and S4). This observation, together with kinetic heterogeneity among discrete insertion events as noted and analyzed previously (Yu et al., 2010; Yudowski et al., 2006), suggests that local surface membrane insertion to dendrites may involve both physical transfer modes.

In any case, retromer-associated endosomes appear to be remarkably resistant to full fusion with the dendritic plasma membrane. Multiple mechanisms are already known to confer specificity on compartmental fusion (Wickner and Schekman, 2008) and we speculate that retromer, perhaps through its associated Bin-amphiphysin-Rvs (BAR) domain proteins that bind to and enforce curvature on endosome membranes (Bonifacino and Hurley, 2008), could confer additional specificity at the subcompartment level by imposing a physical barrier to full endosome fusion. Thus, retromer may function not only to positively select endosome cargoes for rapid surface delivery through recognition by a linked sorting protein such as SNX27, but also to negatively select other endosome-localized cargos that do not engage retromer by preventing full endosome fusion.

In closing, the present observations provide a simple answer to the long-standing and fundamental question that motivated this study: how can neurons deliver selected signaling receptors so rapidly throughout the elaborate dendritic arbor? While retromer-associated endosomes do not exhibit any fixed anatomical relationship to synapses or Golgi elements, they are distributed throughout dendrites in ~2 μm axial intervals and act as local sources of shaft-directed surface insertion events occurring adjacent to them. Based on previous estimates of lateral diffusion rates of β2ARs as well as AMPA receptors in the dendritic plasma membrane (e.g., Araki et al., 2010; Opazo and Choquet, 2011; Yudowski et al., 2006, 2007), this distance is well within the range over which receptors can passively diffuse within several seconds. Thus, retromer-associated endosomes appear to comprise a widely distributed membrane insertion network that places essentially every location of the elaborate dendritic surface within the reach of rapid diffusion.

EXPERIMENTAL PROCEDURES

Constructs and Reagents

Expression constructs are detailed in Supplemental Experimental Procedures. The targeting sequence designed into VPS35 KD constructs was 5′-GAACAT ATTGCTACCAGTA-3′.

Dissociated Neuron Culture and Transfection

Striatal neuron cultures were prepared from embryonic days 18–19 Sprague-Dawley rats (Charles River), transfected with a Nucleofector (Lonza) as described in Kotowski et al. (2011), and imaging was carried out at 7–14 days in vitro (DIV).

Brain Slice Culture and Transfection

Cultured hippocampal slices were prepared from postnatal days 6–9 wild-type rats, transfected after 1 DIV as described in Schnell et al. (2002), and recording was carried out at 7 DIV.

Microscopy and Electrophysiology

Imaging, electrophysiological recording, and data analysis were carried out using standard methods detailed in Supplemental Experimental Procedures.

SUPPLEMENTAL INFORMATION

Supplemental Information includes Supplemental Experimental Procedures, three figures, and four movies and can be found with this article online at http://dx.doi.org/10.1016/j.neuron.2014.02.018.

AUTHOR CONTRIBUTIONS

R.W.-Y.C. and M.P. carried out cell biological experiments, analyzed data, and prepared figures. P.T. carried out preliminary experiments and generated essential shRNA reagents. B.E.H. performed electrophysiological experiments and data analysis. A.M. generated essential rescue constructs. R.A.N. and M.v.Z. designed the study and wrote the manuscript, with input from all authors.

ACKNOWLEDGMENTS

These studies were supported by grants from the NIH (NIDA and NIMH). R.W.-Y.C. received a postdoctoral fellowship from the Croucher Foundation, Hong Kong. M.P. received postdoctoral support from the NIMH. P.T. received a predoctoral fellowship from NSF. B.E.H. received a NARSAD grant from the Brain and Behavior Research Fund. We thank Juan Bonifacino (NIH) for valuable discussion and VPS29-GFP plasmid and Robert Malenka (Stanford) for valuable discussion and pHUGW plasmid. Rapid sequential TIR-FM imaging experiments were carried out in the UCSF Nikon Imaging Center directed by Kurt Thorn, and we thank Dr. Thorn for valuable advice in carrying out these experiments.

Accepted: February 1, 2014
Published: April 2, 2014

REFERENCES

Adesnik, H., Nicoll, R.A., and England, P.M. (2005). Photoinactivation of native AMPA receptors reveals their real-time trafficking. Neuron *48*, 977–985.

Aoki, C., Joh, T.H., and Pickel, V.M. (1987). Ultrastructural localization of beta-adrenergic receptor-like immunoreactivity in the cortex and neostriatum of rat brain. Brain Res. *437*, 264–282.

Araki, Y., Lin, D.T., and Huganir, R.L. (2010). Plasma membrane insertion of the AMPA receptor GluA2 subunit is regulated by NSF binding and Q/R editing of the ion pore. Proc. Natl. Acad. Sci. USA *107*, 11080–11085.

Arighi, C.N., Hartnell, L.M., Aguilar, R.C., Haft, C.R., and Bonifacino, J.S. (2004). Role of the mammalian retromer in sorting of the cation-independent mannose 6-phosphate receptor. J. Cell Biol. *165*, 123–133.

Berg, H.C., and Purcell, E.M. (1977). Physics of chemoreception. Biophys. J. *20*, 193–219.

Bhalla, A., Vetanovetz, C.P., Morel, E., Chamoun, Z., Di Paolo, G., and Small, S.A. (2012). The location and trafficking routes of the neuronal retromer and its role in amyloid precursor protein transport. Neurobiol. Dis. *47*, 126–134.

Bonifacino, J.S., and Hurley, J.H. (2008). Retromer. Curr. Opin. Cell Biol. *20*, 427–436.

Carroll, R.C., Beattie, E.C., Xia, H., Lüscher, C., Altschuler, Y., Nicoll, R.A., Malenka, R.C., and von Zastrow, M. (1999). Dynamin-dependent endocytosis of ionotropic glutamate receptors. Proc. Natl. Acad. Sci. USA *96*, 14112–14117.

Carroll, R.C., Beattie, E.C., von Zastrow, M., and Malenka, R.C. (2001). Role of AMPA receptor endocytosis in synaptic plasticity. Nat. Rev. Neurosci. *2*, 315–324.

Choy, R.W., Cheng, Z., and Schekman, R. (2012). Amyloid precursor protein (APP) traffics from the cell surface via endosomes for amyloid β (Aβ) production in the trans-Golgi network. Proc. Natl. Acad. Sci. USA *109*, E2077–E2082.

Cooney, J.R., Hurlburt, J.L., Selig, D.K., Harris, K.M., and Fiala, J.C. (2002). Endosomal compartments serve multiple hippocampal dendritic spines from a widespread rather than a local store of recycling membrane. J. Neurosci. *22*, 2215–2224.

Herring, B.E., Shi, Y., Suh, Y.H., Zheng, C.Y., Blankenship, S.M., Roche, K.W., and Nicoll, R.A. (2013). Cornichon proteins determine the subunit composition of synaptic AMPA receptors. Neuron *77*, 1083–1096.

Jaiswal, J.K., and Simon, S.M. (2007). Imaging single events at the cell membrane. Nat. Chem. Biol. *3*, 92–98.

Kennedy, M.J., and Ehlers, M.D. (2011). Mechanisms and function of dendritic exocytosis. Neuron *69*, 856–875.

Kennedy, M.J., Davison, I.G., Robinson, C.G., and Ehlers, M.D. (2010). Syntaxin-4 defines a domain for activity-dependent exocytosis in dendritic spines. Cell *141*, 524–535.

Kotowski, S.J., Hopf, F.W., Seif, T., Bonci, A., and von Zastrow, M. (2011). Endocytosis promotes rapid dopaminergic signaling. Neuron *71*, 278–290.

Lauffer, B.E., Melero, C., Temkin, P., Lei, C., Hong, W., Kortemme, T., and von Zastrow, M. (2010). SNX27 mediates PDZ-directed sorting from endosomes to the plasma membrane. J. Cell Biol. *190*, 565–574.

Lissin, D.V., Carroll, R.C., Nicoll, R.A., Malenka, R.C., and von Zastrow, M. (1999). Rapid, activation-induced redistribution of ionotropic glutamate receptors in cultured hippocampal neurons. J. Neurosci. *19*, 1263–1272.

Makino, H., and Malinow, R. (2009). AMPA receptor incorporation into synapses during LTP: the role of lateral movement and exocytosis. Neuron *64*, 381–390.

Opazo, P., and Choquet, D. (2011). A three-step model for the synaptic recruitment of AMPA receptors. Mol. Cell. Neurosci. *46*, 1–8.

Passafaro, M., Piëch, V., and Sheng, M. (2001). Subunit-specific temporal and spatial patterns of AMPA receptor exocytosis in hippocampal neurons. Nat. Neurosci. *4*, 917–926.

Patterson, M.A., Szatmari, E.M., and Yasuda, R. (2010). AMPA receptors are exocytosed in stimulated spines and adjacent dendrites in a Ras-ERK-dependent manner during long-term potentiation. Proc. Natl. Acad. Sci. USA *107*, 15951–15956.

Puthenveedu, M.A., Lauffer, B., Temkin, P., Vistein, R., Carlton, P., Thorn, K., Taunton, J., Weiner, O.D., Parton, R.G., and von Zastrow, M. (2010). Sequence-dependent sorting of recycling proteins by actin-stabilized endosomal microdomains. Cell *143*, 761–773.

Ryan, T.A. (2003). Kiss-and-run, fuse-pinch-and-linger, fuse-and-collapse: the life and times of a neurosecretory granule. Proc. Natl. Acad. Sci. USA *100*, 2171–2173.

Sankaranarayanan, S., De Angelis, D., Rothman, J.E., and Ryan, T.A. (2000). The use of pHluorins for optical measurements of presynaptic activity. Biophys. J. *79*, 2199–2208.

Schnell, E., Sizemore, M., Karimzadegan, S., Chen, L., Bredt, D.S., and Nicoll, R.A. (2002). Direct interactions between PSD-95 and stargazin control synaptic AMPA receptor number. Proc. Natl. Acad. Sci. USA *99*, 13902–13907.

Seaman, M.N., McCaffery, J.M., and Emr, S.D. (1998). A membrane coat complex essential for endosome-to-Golgi retrograde transport in yeast. J. Cell Biol. *142*, 665–681.

Steinberg, F., Gallon, M., Winfield, M., Thomas, E.C., Bell, A.J., Heesom, K.J., Tavaré, J.M., and Cullen, P.J. (2013). A global analysis of SNX27-retromer assembly and cargo specificity reveals a function in glucose and metal ion transport. Nat. Cell Biol. *15*, 461–471.

Steyer, J.A., and Almers, W. (2001). A real-time view of life within 100 nm of the plasma membrane. Nat. Rev. Mol. Cell Biol. *2*, 268–275.

Taraska, J.W., and Almers, W. (2004). Bilayers merge even when exocytosis is transient. Proc. Natl. Acad. Sci. USA *101*, 8780–8785.

Temkin, P., Lauffer, B., Jäger, S., Cimermancic, P., Krogan, N.J., and von Zastrow, M. (2011). SNX27 mediates retromer tubule entry and endosome-to-plasma membrane trafficking of signalling receptors. Nat. Cell Biol. *13*, 715–721.

Wang, X., Zhao, Y., Zhang, X., Badie, H., Zhou, Y., Mu, Y., Loo, L.S., Cai, L., Thompson, R.C., Yang, B., et al. (2013). Loss of sorting nexin 27 contributes to excitatory synaptic dysfunction by modulating glutamate receptor recycling in Down's syndrome. Nat. Med. *19*, 473–480.

Wickner, W., and Schekman, R. (2008). Membrane fusion. Nat. Struct. Mol. Biol. *15*, 658–664.

Yu, Y.J., Dhavan, R., Chevalier, M.W., Yudowski, G.A., and von Zastrow, M. (2010). Rapid delivery of internalized signaling receptors to the somatodendritic surface by sequence-specific local insertion. J. Neurosci. *30*, 11703–11714.

Yudowski, G.A., Puthenveedu, M.A., and von Zastrow, M. (2006). Distinct modes of regulated receptor insertion to the somatodendritic plasma membrane. Nat. Neurosci. *9*, 622–627.

Yudowski, G.A., Puthenveedu, M.A., Leonoudakis, D., Panicker, S., Thorn, K.S., Beattie, E.C., and von Zastrow, M. (2007). Real-time imaging of discrete exocytic events mediating surface delivery of AMPA receptors. J. Neurosci. *27*, 11112–11121.